Strong electron-phonon coupling of the high-energy modes of carbon nanotubes

M. Machón,[1] S. Reich,[2] and C. Thomsen[1]
[1]*Institut für Festkörperphysik, Technische Universität Berlin, Hardenbergstr. 36, 10623 Berlin, Germany*
[2]*Department of Materials Science and Engineering, Massachusetts Institute of Technology, Cambridge, Massachusetts 02139-4307, USA*

(Received 26 July 2006; revised manuscript received 2 October 2006; published 20 November 2006)

We present *ab initio* calculations of electron-phonon coupling matrix elements of the totally symmetric high-energy vibrational modes of carbon nanotubes. The matrix elements depend on nanotube family $(n_1-n_2)\mathrm{mod}\ 3$, chiral angle, and the particular optical transition, similarly to the radial-breathing mode. The strength of the matrix elements of the high-energy mode is up to 6 times higher than for the radial breathing mode. We discuss the implications of our results for the Raman spectrum of nanotubes and for charge carrier relaxation.

DOI: 10.1103/PhysRevB.74.205423 PACS number(s): 78.67.Ch, 71.15.Mb, 63.20.Kr

Electron-phonon coupling is essential for electronic and thermal transport, superconductivity, Raman scattering, luminescence, etc.[1–3] A strong electron-phonon coupling has been long suspected for carbon nanotubes. Their strong Raman signal, which can even be detected for single, isolated tubes, is evidence for this hypothesis.[2,4–6]

A direct comparison of the theory of electron-phonon coupling and experiment is difficult since the experimental information is often integrated over many different phonons. Totally symmetric phonons, however, play a special role in several processes. Intraband charge-carrier relaxations, involved in photoluminescence, can only take place *via* totally symmetric phonons. The large energy difference between the radial breathing mode and the high-energy mode makes the dynamics and probability of the process very different depending on which mode dominates. For this reason it is desirable to know which mode has a stronger coupling.

In the Raman spectrum of nanotubes, due to a combination of the Raman selection rules and the shape depolarization, only totally symmetric modes are observed.[1] These are the radial-breathing mode (RBM) and the two high-energy modes (HEM) derived from the doubly degenerate optical in-plane E_{2g} phonon of graphite. Achiral armchair and zig-zag nanotubes have stronger symmetry restrictions than chiral ones due to the presence of additional symmetry reflection planes. Therefore, for achiral nanotubes, only one of the graphite-derived high-energy modes is totally symmetric, the other being Raman inactive.

Excitation-energy-dependent frequencies, the hallmark of double resonance, were not found in resonant-Raman studies of the radial breathing mode of separated nanotubes.[7–9] The process underlying the HEM, and the origin of its line shape are still controversial.[6,10–12] Both the radial breathing and the high-energy mode, even in the case of double-resonance, stem from the Brillouin zone center or close to it, therefore we study here zone-center phonons.

The optical response of carbon nanotubes is dominated by excitons.[13–16] The coupling of Γ-point phonons to excitons enhances the intensity of the Raman signal. The excitonic levels are bound to the electronic continuum represented in the one-particle picture by bands. Electron-phonon coupling represents an approximation to the exciton-phonon coupling. Coupling between electrons and RBM was studied as a function of diameter, chirality, family, and optical transition by *ab initio* tight-binding calculations.[17–19] First tight-binding results for the HEM were reported recently.[11]

Optical methods are important for the structural determination of carbon nanotubes. The achievement of the chiral-index assignment by these methods raised the question about the chirality distribution present in the samples.[8,20,21] For example, in photoluminescence experiments the zig-zag nanotubes were absent whereas their radial-breathing mode could be measured with Raman spectroscopy.[8,21] The opposite was found for armchair nanotubes. Conclusions about the chirality distribution in samples cannot be made without taking the electron-phonon and optical matrix elements plus exciton relaxation into account.[22]

In this paper we address the question whether a strong chirality dependence can be expected for the HEM-phonon coupling. We calculate *ab initio* the coupling of the totally symmetric high-energy mode(s) of nanotubes with the electrons involved in optical processes, i.e., electrons at the band extrema where the density of states is particularly high. Our calculations yield electron-phonon coupling matrix elements ≈6 times stronger for the HEM than for the radial breathing mode (RBM). The dependence of the matrix elements $\mathcal{M}$ on chirality and so-called family [defined by the value of $(n_1-n_2)\mathrm{mod}\ 3$] is similar to that of the RBM.[17–19]

Calculations were performed with the SIESTA code.[23,24] The parametrization of Perdew and Zunger of the local density approximation was used for the exchange-correlation functional.[25] The core electrons were replaced by nonlocal, norm conserving pseudopotentials.[26] For the valence electrons a singly polarized double-ζ basis of localized atomic orbitals was used.[27] The basis cutoff was determined by localization corresponding to an energy shift of 50 meV. The grid cutoff in real space was 270 Ry. The reciprocal space was sampled with 16 k points except for the (8,4) nanotube, for which only the Γ point was used. Since the (8,4) nanotube is semiconducting with a relatively large band gap of 0.84 eV, we expect the error introduced by sampling the Brillouin zone with one point to remain small. The trends regarding magnitude and sign are unaffected.

The calculated electron-phonon coupling matrix elements $\mathcal{M}_i$ for different nanotubes are shown in Table I. The index i

TABLE I. Diameter d, HEM frequencies (in cm^{-1}) and electron-phonon coupling matrix elements (in meV) of the $A_{1(g)}$ HEM of several nanotubes. For completeness, the frequencies of both HEMs are given for all nanotubes, boldface type indicates the totally symmetric modes. Note that both HEMs of chiral nanotubes are totally symmetric, therefore matrix elements for both modes are given. The index i in $\mathcal{M}_i$ indicates the four first optical transitions for each nanotube. An asterisk indicates a negligible matrix element. The three-dot ellipse indicates it was impossible to extract a matrix element for technical reasons.

	d(Å)	ω^{axial}	ω^{circ}	$\mathcal{M}_1$	$\mathcal{M}_2$	$\mathcal{M}_3$	$\mathcal{M}_4$
(6,6)	8.2	1563	**1626**	−85			
(8,8)	10.9	1564	**1619**	−53	−84	−93	
(11,11)	15.0	1571	**1602**	*	−66	−79	
(8,4)	8.4		**1505**	−31	−22	−25	
(8,4)	8.4	**1670**		71	−66	83	
(6,0)	4.8	**1587**	1490	−152	171		
(10,0)	7.9	**1627**	1590	130	−110	148	151
(15,0)	11.8	**1567**	1579	117	−88	128	134
(17,0)	13.4	**1635**	1613	−89	100	111	−78
(19,0)	15.0	**1635**	1614	94	−83	104	112

runs through the first four optical transitions of each nanotube (see Ref. 17). The strongest matrix element, 171 meV, is found for the second transition of the (6,0) nanotube. This stems from a transition deformation potential of 28 eV/Å (see Ref. 17). We can compare this value with similar calculations performed for MgB_2, a superconducting compound ($T_C \approx 40$ K) with a similar structure as graphene.[28,29] Frozen-phonon calculations of the E_{2g} mode of MgB_2 yield a very strong coupling with Fermi-level electrons, characterized by a deformation potential of 13 eV/Å. The coupling (with optically active quasi-particles) of carbon nanotubes can be even stronger. This can explain why it is possible to measure the Raman signal of an individual nanotube in spite of the small scattering volume.[2,4,6,30]

Comparing zig-zag and armchair nanotubes of similar diameter [compare the (6,6) and (10,0) or the (11,11) and (19,0) nanotubes] we see that the matrix elements for the armchair nanotubes are in general lower. Following the matrix elements for the first optical transition ($\mathcal{M}_1$) of armchair nanotubes we find that their magnitude decreases with diameter. The star for the (11,11) nanotube indicates a negligible matrix element. To understand this node in the coupling strength, we take a look at the electronic band structure of the (11,11) nanotube in Fig. 1(a). We focus our attention on the region of the Brillouin zone where optical absorption in the single-particle picture is most likely to occur, i.e., the maximum of each valence band (k_{abs}) as indicated by the arrows (the absorption between the bands crossing at the Fermi level is forbidden by symmetry). The area of interest, inside the rectangle, is zoomed for clarity in Fig. 1(b). The black solid lines correspond to the equilibrium band structure. The red (gray) lines show the band structure of the nanotube deformed according to the pattern of the A_{1g} HEM with an atomic displacement of 0.01 Å. That means that the

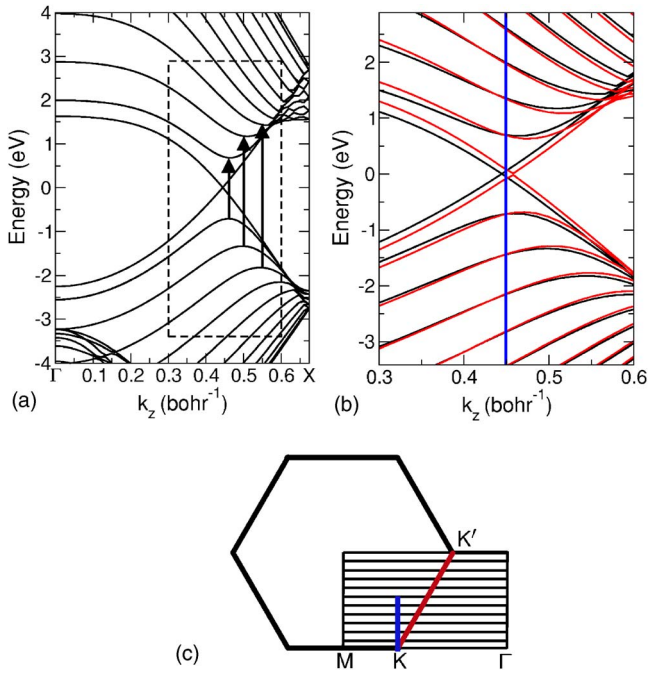

FIG. 1. (Color online) (a) Band structure of an (11,11) nanotube. Arrows indicate the three allowed one-particle optical transitions with lowest energy. The rectangle corresponds to the region shown in panel (b). (b) Solid black lines: electronic bands for the relaxed structure. Red (gray) lines: electronic bands after superimposing the atomic displacements corresponding to the totally symmetric high-energy mode with an amplitude of 0.01 Å. The vertical line indicates the k point where the change of electronic energy is zero (at 2/3 of the Brillouin zone). (c) Brillouin zone of an (11,11) nanotube (parallel black lines) mapped onto the Brillouin zone of graphite. The red (gray) line along the edge of the hexagon indicates approximately the position of the band extrema of armchair nanotubes. The blue (gray) line indicates the region of the node in the electron-phonon coupling.

change of energy of a particular electronic state is proportional to the electron-HEM coupling deformation potential for that state. The vertical line indicates a point in the BZ where the deformation potential is negligible. Graphically, a vanishing matrix element occurs at the intersection of displaced and undisplaced bands. This node appears for all armchair nanotubes, at two thirds of the BZ for the lowest transition energies. As the diameter of the nanotube grows k_{abs} moves closer and closer to two thirds of the BZ and therefore the electron-phonon coupling vanishes for the lower transitions of large-diameter armchair nanotubes. The first transition of the (11,11) nanotube in our calculation is at 1.4 eV, which can serve as an estimate of the lowest energy at which the high-energy mode of armchair nanotubes can be observed. The node in the electron-phonon coupling matrix element and the maxima and minima of the electronic bands correspond to different lines in the graphene Brillouin zone. The band extrema of armchair nanotubes can be mapped approximately onto the the KK' direction indicated in Fig. 1(c) in red (gray). A vanishing electron-phonon coupling is found at the line perpendicular to the ΓKM direction going through the K point [blue (gray) line in the figure]. The de-

creasing coupling of electrons to the HEM with diameter and the increasing coupling with transition index thus have the same origin. They can be traced back to the electron-phonon coupling of graphene.

Returning to Table I we look now at the matrix elements of a zig-zag nanotube, for example the (17,0). $\mathcal{M}_1$ and $\mathcal{M}_4$ are positive and $\mathcal{M}_2$ and $\mathcal{M}_3$ negative, and their absolute value is larger. A sign alternation is observed for all zig-zag nanotubes. Similarly to the RBM relative magnitude and sign of $\mathcal{M}_i$ are explained by zone folding of the graphite phonon-induced electronic band distortion. For the same transition energy the sign of the matrix element depends on the family of the nanotube as defined by the value of $\nu=(n_1-n_2)\mathrm{mod}\,3$. This behavior was also found for the radial-breathing mode and is in good agreement with experiment.[9,17]

We also calculated the electron-phonon coupling matrix elements for both A_1 high-energy modes of the (8,4) chiral nanotube. In the case of chiral nanotubes the high-energy totally symmetric modes are not strictly axial or tangential since they belong to the same irreducible representation and have similar frequencies, which allows their mixing.[31] Calculations show, however, that this deviation is small even for narrow nanotubes.[32] As can be seen in Table I the trends observed for achiral tubes are also present: the tangential matrix elements are lower than the axial ones. The latter have sign alternations, but are lower than those of the (10,0) nanotube with a similar radius.

The dependence of the electron-phonon coupling on phonon type, nanotube chiral angle and diameter should be reflected in the Raman spectra of carbon nanotubes. First, we expect the intensity of the RBM in resonance to be much lower than that of the HEM. Furthermore, we expect armchair nanotubes to give a weaker HEM signal than zig-zag tubes. In particular, the signal from armchair nanotubes will tend to disappear for lower excitation energies. For similar chiral angle the intensity of nanotubes belonging to $\nu=+1$ families will be different from the intensity of -1 tubes, since the Raman efficiency is proportional to $|\mathcal{M}|^2$. In metallic zig-zag tubes, with transitions grouped in pairs with very similar energies, we expect intensity differences between both transitions in a pair. See, for example, the ratio $|\mathcal{M}_1/\mathcal{M}_2|^2\approx 2$ for the (15,0) nanotube. For an experimental confirmation Raman measurements of isolated nanotubes in full resonance are necessary including an (n_1,n_2) assignment, e.g., by electron diffraction or a unique identification *via* the experimental Kataura plot.[8,9,20] The alternation in sign for close-lying pairs of transition energies in metallic tubes gives rise to Raman interferences as observed for the RBM by Bussi *et al.*[33]

The strength of the coupling of the electrons at k_{abs} to the HEM is much stronger than to the RBM. This has consequences for the electronic relaxation after optical absorption. The HEM dominates photorelaxation, which implies more efficient relaxation than by emission of radial-breathing mode phonons. With an energy ratio of ≈ 8 (the factor depending on the nanotube diameter) the relaxation via the HEM needs 8 times less emission steps than the relaxation *via* the radial breathing mode. Htoon *et al.*[34] measured photoluminescence excitation spectra of individual nanotubes. In their spectra photoluminescence traces as well as Raman traces can be found. When these cross, the signal is enhanced. They find at these spots a double signal: a narrow resonant Raman signal and a broad luminescence band, enhanced by a phonon-assisted transition. The phonon-assisted transitions are as intense as the resonant photoluminescence peaks, and even third-order processes are found. This indicates a very strong overall exciton-phonon coupling in agreement with our calculations.

Hagen *et al.*[35] measured the photoluminescence lifetime of single-walled nanotubes on a substrate. The dependence of the decay time on temperature of the (6,4) nanotube could be explained with a model including strong coupling with the radial breathing mode. This nanotube has a chiral angle of 23° which is close to armchair. The photoluminescence was measured at ≈ 1.4 eV, which coincides with the threshold we predicted for the high-energy mode, therefore emission of radial-breathing mode phonons is the main relaxation path. This is not necessarily true for other chiral angles and transition energies as shown in Fig. 1.

In pump-probe experiments, coherent phonons can be activated and observed. Such measurements have shown the radial breathing mode of several nanotubes.[36,37] Measurements with higher temporal resolution also show the high-energy mode.[38] This is again an indication of strong electron-phonon coupling of these modes.

In summary, we presented calculations of the totally symmetric high-energy phonon modes of carbon nanotubes. We obtain family-dependent sign alternation, stronger coupling for zig-zag than for armchair nanotubes, and a dependence on the particular transition, similarly to the radial breathing mode.[11] For chiral nanotubes a zig-zag and an armchairlike behavior can be expected for the mainly axial and mainly tangential modes, respectively. The magnitude of the coupling is about 6 times stronger for the HEM than for the RBM.

[1] S. Reich, C. Thomsen, and J. Maultzsch, *Carbon Nanotubes, Basic Concepts and Physical Properties* (Wiley-VCH, Berlin, 2004).

[2] M. Oron-Carl, F. Hennrich, M. Kappes, H. v. Löhneysen, and R. Krupke, Nano Lett. **5**, 1761 (2005).

[3] M. S. Strano, S. K. Doorn, E. H. Haroz, C. Kittrell, R. H. Hauge, and R. E. Smalley, Nano Lett. **3**, 1091 (2003).

[4] G. S. Duesberg, I. Loa, M. Burghard, K. Syassen, and S. Roth, Phys. Rev. Lett. **85**, 5436 (2000).

[5] A. Jorio, R. Saito, J. H. Hafner, C. M. Lieber, M. Hunter, T. McClure, G. Dresselhaus, and M. S. Dresselhaus, Phys. Rev. Lett. **86**, 1118 (2001).

[6] J. Maultzsch, S. Reich, U. Schlecht, and C. Thomsen, Phys. Rev. Lett. **91**, 087402 (2003).

[7] C. Thomsen and S. Reich, Phys. Rev. Lett. **85**, 5214 (2000).
[8] H. Telg, J. Maultzsch, S. Reich, F. Hennrich, and C. Thomsen, Phys. Rev. Lett. **93**, 177401 (2004).
[9] J. Maultzsch, H. Telg, S. Reich, and C. Thomsen, Phys. Rev. B **72**, 205438 (2005).
[10] M. Lazzeri, S. Piscanec, F. Mauri, A. C. Ferrari, and J. Robertson, Phys. Rev. B **73**, 155426 (2006).
[11] V. N. Popov and P. Lambin, Phys. Rev. B **73**, 165425 (2006).
[12] K. Kempa, Phys. Rev. B **66**, 195406 (2002).
[13] C. L. Kane and E. J. Mele, Phys. Rev. Lett. **90**, 207401 (2003).
[14] C. D. Spataru, S. Ismail-Beigi, L. X. Benedict, and S. G. Louie, Phys. Rev. Lett. **92**, 077402 (2004).
[15] F. Wang, G. Dukovic, L. E. Brus, and T. F. Heinz, Science **308**, 838 (2005).
[16] J. Maultzsch, R. Pomraenke, S. Reich, E. Chang, D. Prezzi, A. Ruini, E. Molinari, M. S. Strano, C. Thomsen, and C. Lienau, Phys. Rev. B **72**, 241402(R) (2005).
[17] M. Machón, S. Reich, H. Telg, J. Maultzsch, P. Ordejón, and C. Thomsen, Phys. Rev. B **71**, 035416 (2005).
[18] V. N. Popov, L. Henrard, and P. Lambin, Phys. Rev. B **72**, 035436 (2005).
[19] S. V. Goupalov, Phys. Rev. B **71**, 153404 (2005).
[20] C. Fantini, A. Jorio, M. Souza, M. S. Strano, M. S. Dresselhaus, and M. A. Pimenta, Phys. Rev. Lett. **93**, 147406 (2004).
[21] S. M. Bachilo, M. S. Strano, C. Kittrel, R. H. Hauge, R. E. Smalley, and R. B. Weisman, Science **298**, 2361 (2002).
[22] S. Reich, C. Thomsen, and J. Robertson, Phys. Rev. Lett. **95**, 077402 (2005).
[23] P. Ordejón, E. Artacho, and J. M. Soler, Phys. Rev. B **53**, R10441 (1996).
[24] J. M. Soler, E. Artacho, J. D. Gale, A. García, J. Junquera, P. Ordejón, and D. Sánchez-Portal, J. Phys.: Condens. Matter **14**, 2745 (2002).
[25] J. P. Perdew and A. Zunger, Phys. Rev. B **23**, 5048 (1981).
[26] N. Troullier and J. L. Martins, Phys. Rev. B **43**, 1993 (1991).
[27] J. Junquera, O. Paz, D. Sánchez-Portal, and E. Artacho, Phys. Rev. B **64**, 235111 (2001).
[28] J. Nagamatsu, N. Nakagawa, T. Muranaka, Y. Zenitani, and J. Akimitsu, Nature (London) **410**, 63 (2001).
[29] J. M. An and W. E. Pickett, Phys. Rev. Lett. **86**, 4366 (2001).
[30] M. Paillet, P. Poncharal, A. Zahab, J.-L. Sauvajol, J. C. Meyer, and S. Roth, Phys. Rev. Lett. **94**, 237401 (2005).
[31] S. Reich, C. Thomsen, and P. Ordejón, Phys. Rev. B **64**, 195416 (2001).
[32] I. Milošević, E. Dobardžić, and M. Damnjanović, Phys. Rev. B **72**, 085426 (2005).
[33] G. Bussi, J. Menéndez, J. Ren, M. Canonico, and E. Molinari, Phys. Rev. B **71**, 041404(R) (2005).
[34] H. Htoon, M. J. O'Connell, S. K. Doorn, and V. I. Klimov, Phys. Rev. Lett. **94**, 127403 (2005).
[35] A. Hagen, M. Steiner, M. B. Raschke, C. Lienau, T. Hertel, H. Qian, A. J. Meixner, and A. Hartschuh, Phys. Rev. Lett. **95**, 197401 (2005).
[36] C. Manzoni, A. Gambetta, E. Menna, M. Meneghetti, G. Lanzani, and G. Cerullo, Phys. Rev. Lett. **94**, 207401 (2005).
[37] Y. S. Lim, K. Y. Yee, J. H. Kim, J. Shaver, E. H. Haroz, J. Kono, S. K. Doorn, R. H. Hauge, and R. E. Smalley, Nano Lett. (to be published).
[38] A. Gambetta, C. Manzoni, E. Menna, M. Meneghetti, G. Cerullo, G. Lanzani, S. Tretiak, A. Piryatinsky, R. L. Martin, and A. R. Bishop, Nat. Phys. **2**, 515 (2006).